Experimental Study on Thermoelectric Energy Harvesting using the Temperature Distribution on Bridge Components

Kouichi Takeya
Assistant Prof., Dept. of Civil and Environmental Engineering, University of Yamanashi, Kofu, Japan

Mizuki Irie
Graduate Student, Dept. of Civil and Environmental Engineering, Tokyo Institute of Tech., Tokyo, Japan

Eiichi Sasaki
Associate Prof., Dept. of Civil and Environmental Engineering, Tokyo Institute of Tech., Tokyo, Japan

ABSTRACT: To secure power supplies is a critical problem for bridge health monitoring (BHM), and energy harvesting has attracted attention in recent years as one solution to this problem. We focused on the temperature distribution in bridge components which influences the structural behavior of bridges. The thermoelectric energy harvesting uses the Seebeck effect and converts temperature differences into electricity. As a fundamental study on the thermoelectric energy harvesting using the temperature distribution on bridge components, temperature measurements on an existing steel girder bridge was carried out. The appropriate components of bridges and installation locations for high conversion efficiency of energy harvesting were discussed from the results. Abilities of a prototype thermoelectric generator were tested, and the characteristic curves between power generation and temperature differences were formulated. Finally, the harvesting energy was estimated by using the characteristic curves of the thermoelectric generator and the measured temperature on the target bridge.

1. INTRODUCTION

Various structures have been built after the 1950s, and according to the research by the Ministry of Land, Infrastructure, Transport and Tourism, 67% of all 730 thousand road bridges over two meters in Japan will be 50 years or older in 2033. The guideline under the ministerial ordinance was published in 2014 to maintain the serviceability of road bridges; it requires the periodic inspection of every five years. However, the significant inspection in all road bridges would not be sustainable due to the reduction of workforce and maintenance budget. As a solution method, the bridge health monitoring (BHM), which quantitatively evaluates the condition of bridges from analyzing structural responses or circumstances with various sensors, has been focused. However, to secure long-term power supply of the system is a critical problem for BHM.

As one method of securing power supply, energy harvesting has attracted attention in recent years, such as vibration-based energy harvesting of bridges. Yoshida developed a piezo type energy harvester for railway bridges and examined its performance on an actual railway bridge, Yoshida et al. (2014). Takeya proposed the electromagnetic energy harvesting for road bridges using tuned mass systems from theoretical approaches and numerical analysis, Takeya and Sasaki (2015) and Takeya et al. (2016). The proposed electromagnetic energy harvester was developed, and its ability was demonstrated in the experiment on an existing highway bridge, Takeya et al. (2016). Although the vibration-based energy harvesting for bridges has been studied in the last decade, it is difficult to harvest

vibration energy from bridges with low traffic volume so far.

From the circumstance described above, we focused on the thermal energy source stored in bridge components. Several studies showed that temperature differences occur continuously in bridge components because of the difference in heat capacities of materials, Kobayashi et al. (2002). The thermoelectric generator using the Seebeck effect has been developed mainly for harvesting waste heat in factories, Kiziroglou et al. (2016). The thermoelectric generator can continuously generate electricity from heat flow across a temperature gradient. The surface temperature is different between bridge decks and girders by several degrees due to differences in materials, and it influences the structural behavior of bridges. Besides, power saving technology of sensors and wireless communication has been developed rapidly in recent years. Therefore, thermoelectric power generation can be expected as a continuous power source of BHM systems. Moreover, it would measure the temperature distribution of bridge components using its generated voltage.

In this study, as a fundamental study on thermoelectric energy harvesting from a temperature gradient in bridge components, temperature distribution in an existing bridge was measured, and specific tests of thermoelectric generators were carried out. Based on measured data, the possibility of thermoelectric generation using temperature differences in bridge components was discussed.

2. FIELD MEASUREMENTS

2.1. Target bridge

In the field measurements, at first, in order to investigate temperature change characteristics in bridge components, temperature measurements were conducted from March to August in 2018. The target bridge is a road bridge located in Kofu city in Yamanashi prefecture, and it consists of a concrete deck and I-shaped steel girders shown in Figure 1. Three cross-sections in the bridge were selected for the measurements at the bridge end, the first span, and the second span. Figure 2 shows the measuring locations at the bridge end cross-section. Twelve thermometers attached on the bridge components measured the surface temperature (red squares), and other three thermometers measured the air temperature nearby bridge components (blue squares). Figure 3 shows the pictures of attached sensors on the measuring locations.

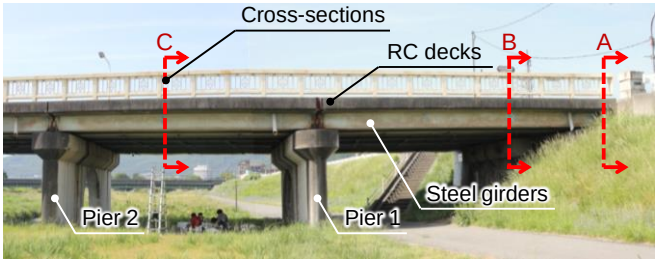

Figure 1: An overview picture of the target bridge.

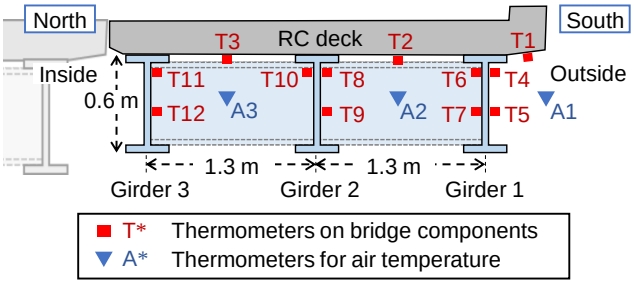

Figure 2: Sensor locations at a cross-section.

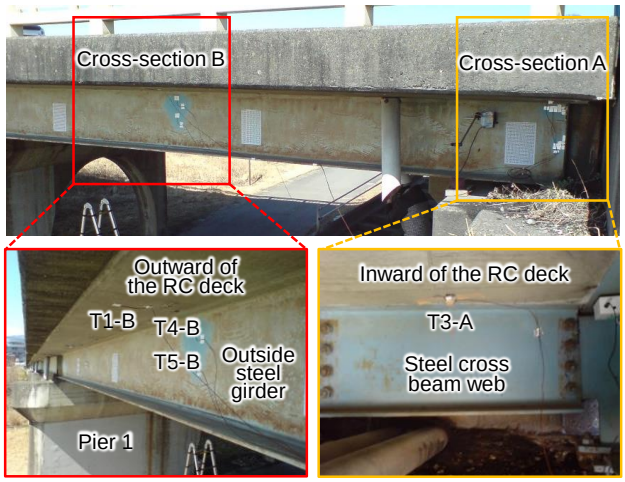

Figure 3: Pictures of attached thermometers on the measuring locations.

2.2. Temperature distribution

Temperature distribution on the bridge components was measured using an infrared

thermographic camera (FLIR SC640). Figure 4 shows the images taken from a backside of RC (reinforced concrete) decks, steel girders, and an RC bridge pier. Figure 5 shows the outer steel girder and RC floorboard of the target bridge looking upward from directly below. The red frames in the left are the ranges of the infrared thermography. These images were taken in 6th Mars 2018 from 11:40 to 12:20, the weather was bright. According to the data of the meteorological observatory located around 1 km from the target bridge, the temperature and the humidity at 12:00 were 12.4 ºC and 37 %, respectively.

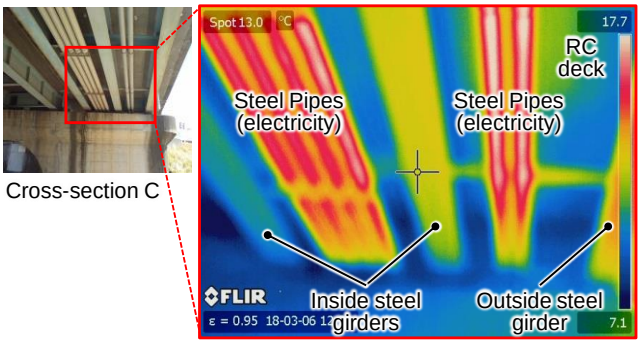

Figure 4: Temperature distribution of the backside of RC decks and steel girders near cross-section C.

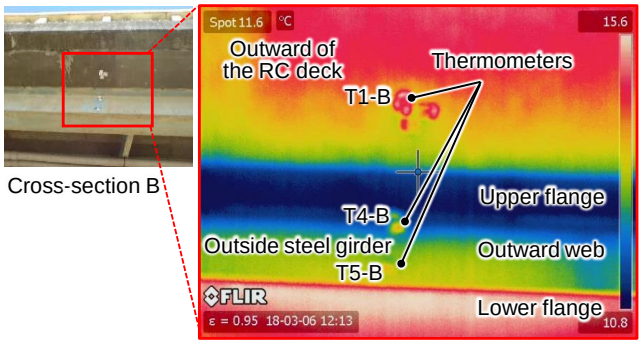

Figure 5: Temperature distribution of the outward of the RC deck and the outside girder near cross-section B.

The right side in Figure 4 is on the south, and it was found that the surface temperature of the lower flange of the two steel girders on the south side among the three was higher than another. From Figure 5, the back side of the RC deck and the bottom surface of the lower flange of the steel girder are around 15 ºC, and the lower side of the upper flange is around 11 ºC. In particular, the temperature difference between the upper flange and the lower flange of the steel girder on the south side was around 5 ºC. The reason for the relatively high temperature of the bottom surface of the lower flange is the influence of reflected solar radiation from the river bed and infrared radiation since RC decks shaded the steel girders from the solar radiation. On the other hand, the main reason for the high temperature of the RC deck is considered that the heat on the concrete pavement surface due to direct solar radiation is transmitted.

There are two approaches to obtain the temperature gradient in the generators considering the application of thermoelectric generators to bridges. One approach is the temperature difference between bridge components and the air, and another is the temperature difference between two different components of bridges. In general, temperature gradient decreases in proportion to distance; i.e., a conversion efficiency of thermoelectric generation decreases with distance. By the former approach, both surfaces of thermoelectric generators are attached on bridge components and the air through heat sinks and thermal glue, energy loss against distance is therefore minimum. On the other hand, by the latter approach, it is difficult so far to attach the thermoelectric generators on different bridge components with low energy loss, such as the RC deck and steel girders. Therefore, in this study, the approach using the temperature difference between bridge components and the air was selected and considered hereafter.

2.3. Temperature-time history of bridge components

Figure 6 shows time history of the surface temperature on the backside and outward of the RC deck in the cross-section B, where the measuring location is T1-B in Figure 2. Figure 7 shows that on the outside girder at T5-B from 10th to 11th July 2018. Surface temperatures of the steel girder changed along with the air temperature, whereas that of RC deck delayed and gradually changed against the air temperature. Notably, the

RC deck kept its temperature higher over 4 ºC during the night against the air. The absolute temperature difference of the outward of RC decks against the air was, therefore, more significant than that of the outside steel girder. It is considered that this temperature difference derives from the difference in heat capacity and location of bridge components. The thermal capacity of RC decks is higher than that of steel girders; moreover, RC decks receive solar radiation directly or through pavements.

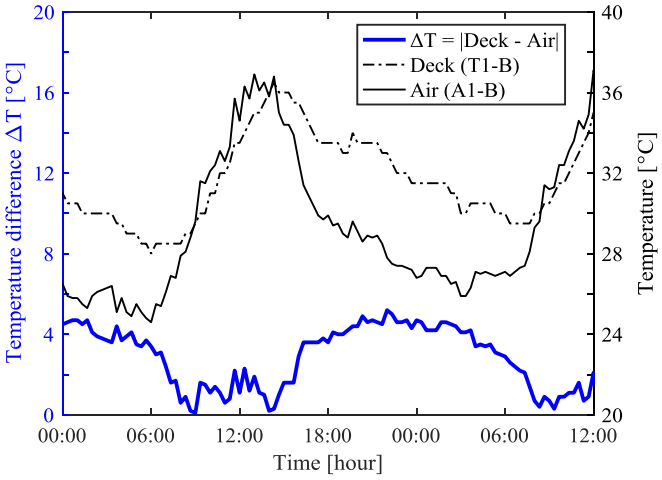

Figure 6: Time history of the temperature of the outward of the RC deck (T1-B) and the air on 10th and 11th July 2018.

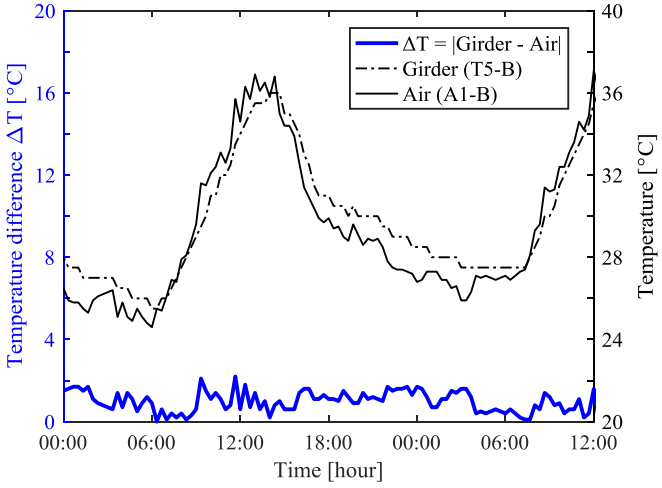

Figure 7: Time history of the temperature of the outside steel girder (T5-B) and the air on 10th and 11th July 2018.

Through measurements in the existing bridge, it was revealed that the high heat capacity and the location of bridge components are essential to keep the temperature difference higher. RC decks are therefore appropriate to satisfy the requirements.

Figure 8 shows time history of the surface temperature on the backside and outward of the RC deck in the cross-section A (T1-A), where the measuring location is T1-A, the air temperature at A1-A, and the temperature difference between them from 7th to 14th March 2018. Surface temperatures of the RC deck increased during the morning and recorded the peak value at around 15:00. Increasing rate of the surface temperature of the RC deck was lower than that of air, and the peak time was delayed by dozens of minutes from that of air temperature. After the evening and in the night, surface temperatures of the RC deck decreased gradually although the air temperature rapidly fell. The absolute temperature difference between surfaces of RC decks and the air had, therefore, two peaks in a day and occurred continuously.

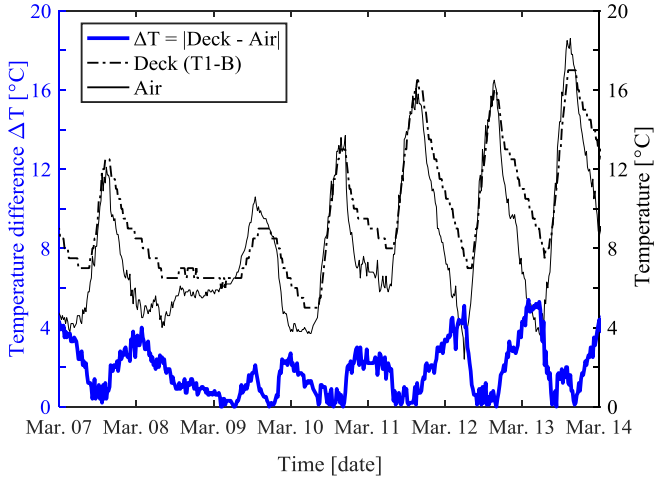

Figure 8: Time history of the temperature of the outward of the RC deck (T1-B) and the air from 7th to 14th March 2018.

Based on these results, it is considered that the temperature difference between the RC deck and the air does not depend on the seasons, but depends on the climate; it increases with the temperature difference between daytime and night since the RC deck stores the thermal energy.

3. SPECIFIC TESTS

3.1. Methods and equipment

Thermoelectric generators use the Seebeck effect and consist of thermoelectric semiconductors. Thermal energy harvesting using thermoelectric generators is mainly intended for waste heat from factories such as tens to hundreds degrees Celsius. Thus, the energy harvesting performance against a temperature difference of several degrees Celsius is still unknown. In this section, experiments were conducted to evaluate the performance of thermoelectric energy harvesting.

A prototype thermoelectric generator was sandwiched between an aluminum heat sink and a base plate. The aluminum base plate was heated by adjusting the power consumption of the two cement resistors. Thermal glue (silicone grease) was used to bond two type T thermocouples to the center of the lower surface of the base plate and the center of the upper surface of the heat sink, respectively.

The prototype thermoelectric generator was connected to a current sense resistor and a variable resistor in series. The electro-motive force and current were measured when the temperature difference was induced to both surfaces of the thermoelectric generator. Ohm's law calculated the current from the voltage measurement at the current sense resistor. Table 1 shows specifications of the equipment used in the experiment. Measuring object and resolution of the measured data is shown in Table 2.

Table 1: Specifications of the equipment used in specific tests of the thermoelectric generator.

Prototype thermoelectric generator	Electric resistance: 2.24 Ω (27 ºC) Thermal resistance: 1.066 ºC/W Size: 48×56.5×1.35 mm
Data logger	NR-600, NR-TH08 (Keyence Co.)
Temp. sensors	Thermocouples (Type T)
Current sensor	Current sense resistor (1 Ω ± 1 %)
Heaters	Cement resistors (10 W×2)
Thermal glue	Silicone grease (0.84 W/m/K)

Table 2: Resolution of the measured data in specific tests of the prototype thermoelectric generator.

Measuring object	Resolution
Base aluminum plate	0.01 ºC
Heat sink	0.01 ºC
Electro-motive force	0.01mV
Current	0.01mA

3.2. Experimental results and formulation

As shown in Figure 9, the measured time history data of the temperature difference, generated voltage and current were slightly changed in time, although the measurement was carried out after when the temperature reached equilibrium. The temperature difference fluctuates in the range of about ± 0.1 ºC, and influence the generated voltage and current slightly. Therefore, designate the temperature difference and read the voltage and current when the designated temperature difference was measured and plot them on the graph (Figure 10).

If there is more than one corresponding data, the average value is used. The relationship between the generated voltage and current for each temperature difference is shown in Figure 11 with blue points on the left axis, and the relationship between the generated electric power and current is plotted with red points on the right axis. The blue lines are obtained from the relationship between the generated voltage and current by the least squares method. The red dotted line shows the quadratic curves obtained from the relationship between the generated power and current by the least squares method.

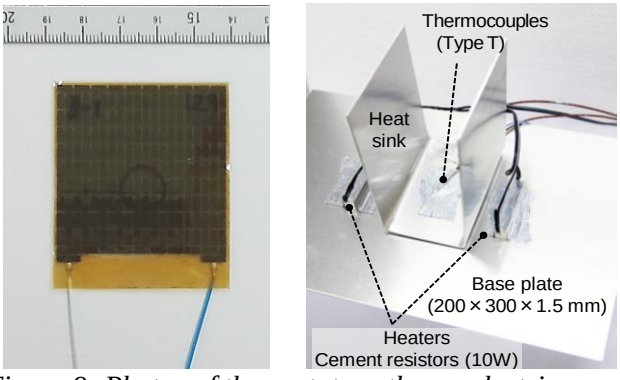

Figure 9: Photos of the prototype thermoelectric generator (left) and specific tests (right).

The following equation explains the blue lines, and the coefficients are as shown in Table 3.

$$E(I, \Delta T) = -\alpha I + \beta(\Delta T) \quad (1)$$

Where E is the generated voltage [mV], and I is current [mA]. Here, the coefficient α is considered to be constant regardless of the temperature difference, and the average is α = 3.2429 [V/A]. On the other hand, β indicates the electromotive force (EMF: the electrical potential when no current is flowing) [mV] and depends on the temperature difference.

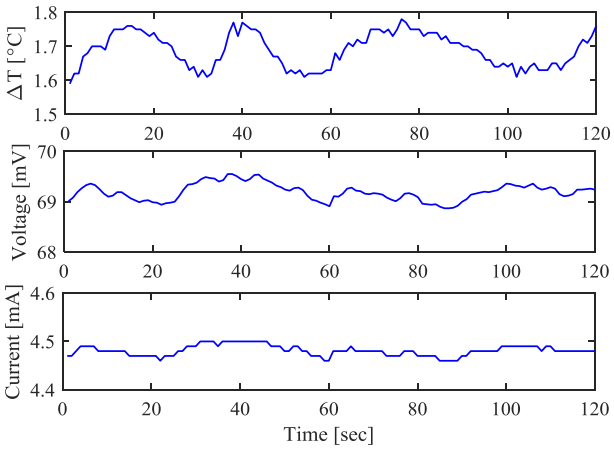

Figure 10: Time history of the temperature difference, voltage, and current in specific tests.

Table 3: Parameter values of relationship between voltage and current of the thermoelectric generator.

ΔT	0.40ºC	0.65ºC	1.00ºC	1.70ºC	Normalized
α	3.2041	3.3145	3.2446	3.2085	3.2429 (average)
β	23.239	36.099	53.794	86.227	$\beta(\Delta T)$

The right axis in Figure 11 shows generated power, which is calculated by multiplying voltage and current. The power generation efficiency is maximized when the generated power is the maximum; i.e., the generated voltage which gives the maximum efficiency is half of the electromotive force.

Since the electromotive force $\beta(\Delta T)$ is assumed to be proportional to the temperature difference ΔT, the electromotive force divided by the temperature difference is considered and shown in Figure 12. However, against expectations, the electromotive force divided by the temperature difference $\beta(\Delta T)/\Delta T$ is not a constant value but still has a dependency on the temperature difference. When the temperature difference is very small as 0.4 ºC, the variation when divided by the temperature difference becomes large (± 10 mV/K). Therefore, this point was excluded, and an approximate straight line was obtained by the least squares method.

$$\beta(\Delta T)/\Delta T = -\gamma \Delta T + \delta \quad (2)$$

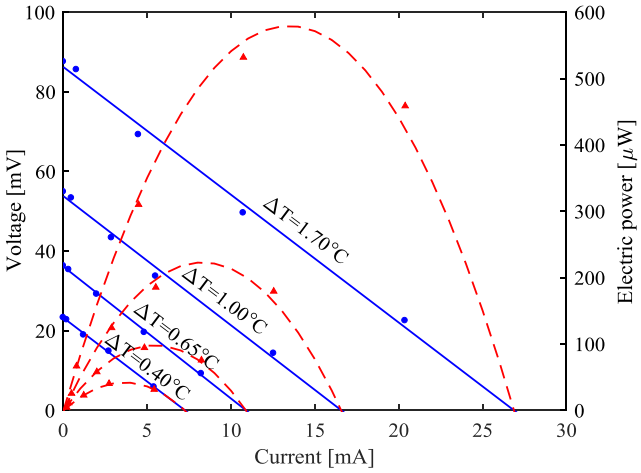

Figure 11: The characteristic curve of the generated voltage, current, and power under temperature differences.

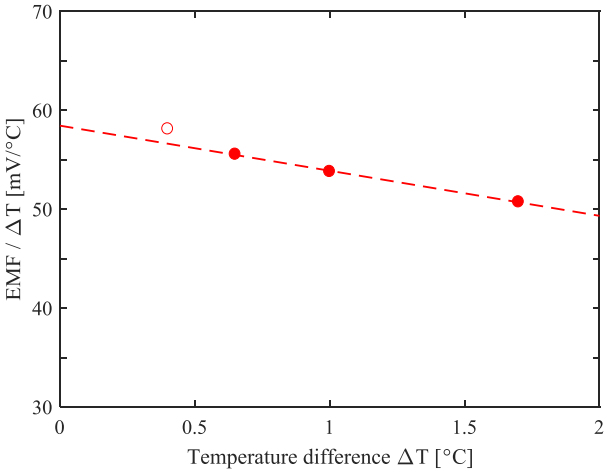

Figure 12: The characteristic curve of the electromotive force divided by the temperature difference against the temperature difference.

Where, γ = 4.5578 [mV/K^2], δ = 58.4403 [mV/K]. From the above, the electromotive force can be expressed by the quadratic equation of the temperature difference as follows.

$$\beta(\Delta T) = -\gamma \Delta T^2 + \delta \Delta T \quad (3)$$

The generated voltage and power can be summarized as follows

$$E(I, \Delta T) = -\alpha I - \gamma \Delta T^2 + \delta \Delta T \quad (4)$$

We note that the generated voltage which gives the maximum efficiency, named hereafter the optimum generated voltage E^*, is half of the electromotive force; $E^*(\Delta T) = 0.5\beta(\Delta T)$ and the optimum current $I^*(\Delta T) = 0.5\alpha^{-1}\beta(\Delta T)$. Therefore, the optimum electrical load R^* [Ω] and the generated electric power W^* [μW] are

$$R^* = \alpha \quad (5)$$

$$W^*(\Delta T) = 0.25a^{-1}\Delta T^2(-\gamma \Delta T + \delta)^2 \quad (6)$$

We note that the above equation would be applied when the temperature difference ΔT is up to several degrees Celsius.

4. ESTIMATION OF THERMOELECTRIC ENERGY HARVESTING ON THE BRIDGE

4.1. Analysis target

To estimate the harvesting energy, we used the measured temperature difference between bridge components and the air from 7th to 14th July 2018. The optimum electric load R^* which gives the highest harvesting power was described in the previous chapter; it equals α in Table 3. Eq. (6) calculates the maximum harvesting energy from time histories of the temperature difference. To consider the difference in location and bridge components for thermoelectric generation, we selected the measured surface temperature at three locations; the outward of RC decks at T1-A in the cross-section A, the inward of RC decks between two girders at T3-B and the outward of the outside steel girder at T5-B in the cross-section B, respectively (explained in Figure 2). The analyzed air temperature was measured at the nearest measuring points from the selected three locations of bridge components.

4.2. Estimated harvesting energy

Figure 13 shows the time history of the temperature difference between the selected locations of bridge components and the air at the nearest measuring points from these locations. On 7th and 8th July 2018, the peaks of the temperature difference on the outward of RC decks was higher than that on the inward of RC decks. On the other hand, the temperature difference on both locations of RC decks was similar during 10th to 13th July. It is assumed that the amount of solar radiation affected these differences. According to the data at Kofu meteorological observatory, the total time of the solar radiation per day was around two hours or less on 7th and 8th July, although it was longer than four hours on the other days.

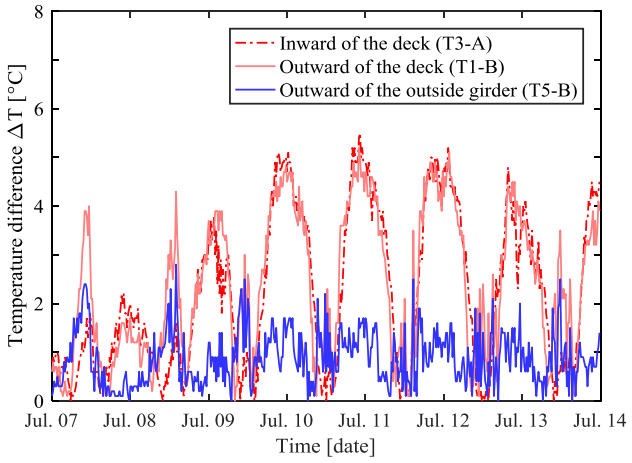

Figure 13: Time history of the temperature difference at the selected location and bridge components.

The harvesting energy at the selected locations by applying the thermoelectric generator was calculated and shown in Figure 14. It was estimated that the location at the outward of RC decks induced the highest harvesting energy among the three locations except on 11th July. It was experimentally assumed that the harvesting energy per day is dozens of mWh if the thermoelectric generator is applied on RC decks. The generated electric energy seems to be a practical level since the power consumption of low-power sensors applied in bridge health

monitoring is mW or less. However, it is necessary to use booster circuits or connect thermoelectric generators in series to increase the generated voltage. We should note that the estimated harvesting energy is ideal values without considering the finiteness of heat capacity of the bridge components and the air, and heat loss especially between the air and the thermoelectric generator. The size and configuration of heat sinks are therefore essential parameters for minimizing the heat loss.

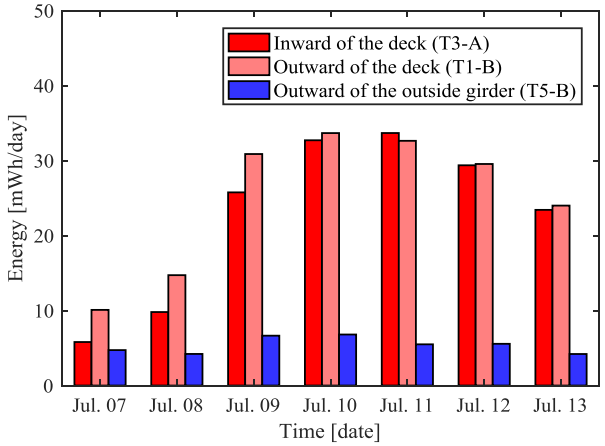

Figure 14: Comparison of the estimated harvesting energy at the selected location and bridge components.

5. CONCLUSIONS

In this study, to propose a thermoelectric energy harvesting for bridges, the field measurements in the existing road bridge and the specific tests were carried out to clarify the appropriate installation location of thermoelectric generators. The temperature distribution in the bridge components was analyzed and the harvesting energy was estimated from the results. The findings are as follows.

- The surface temperature of bridge members is mainly influenced not only by direct solar radiation but also reflective and infrared radiation from the ground surface. RC decks induce the temperature difference against the air because of their large thermal capacity and low thermal conductivity.
- By considering the measured temperature distribution and the distance among bridge components, the air-cooling effect using heat sinks was selected to obtain the temperature difference on both surfaces of thermoelectric generators.
- Relationships between the temperature difference and generated voltage, current and power were formulated through specific tests of the thermoelectric generator.
- The harvesting energy was estimated from the temperature difference between the selected bridge components and the air measured in the field measurement. The outward of RC decks induced the maximum estimated harvesting energy of dozens of mWh per day.

Further investigation is necessary to realize the thermoelectric power generation in bridges; the practical configuration of the thermoelectric generators and installation methods and locations through field measurements and application.

6. REFERENCES

Yoshida,Y., Kobayashi, Y. and Uchimura, T. (2014), "Development of the Monitoring System that Operates with the Power Generated from the Bridge Vibration", Journal of JSCE, Ser. A1 (Structural Engineering & Earthquake Engineering (SE/EE)), Vol.70, No.2, 282-294.

Takeya, K., and Sasaki,E. (2015), "Characteristics Investigation of Tuned Mass Energy Harvester for Bridge Vibration", Journal of JSCE, Ser. A1 (Structural Engineering & Earthquake Engineering (SE/EE)), Vol.71, No.2, 267-276.

Takeya, K., Sasaki, E. and Kobayashi, Y. (2016), "Design and parametric study on energy harvesting from bridge vibration using tuned dual-mass damper systems", Journal of Sound and Vibration, Vol. 361, 50-65.

Kobayashi, Y., Miki, C., Deno, M. and Saito, K. (2002), "Deformation of Composite Girder Bridge due to Temperature for Bridge Health Monitoring", Journal of Structural Engineering, JSCE, Vol.48A, 979-985.

Kiziroglou, M., E., Becker, Th., Wright, S., W., Yeatman, E., M., Evans, J., W. and Wright, P. K. (2016), "Thermoelectric Generator Design in Dynamic Thermoelectric Energy Harvesting", Journal of Physics, Vol. 773.